Fermi Surface and Quasiparticle Excitations of Overdoped $Tl_2Ba_2CuO_{6+\delta}$

M. Platé,[1] J. D. F. Mottershead,[1] I. S. Elfimov,[1] D. C. Peets,[1] Ruixing Liang,[1] D. A. Bonn,[1] W. N. Hardy,[1] S. Chiuzbaian,[2] M. Falub,[2] M. Shi,[2] L. Patthey,[2] and A. Damascelli[1]

[1]*Department of Physics and Astronomy, University of British Columbia, Vancouver, British Columbia V6T 1Z1, Canada*
[2]*Swiss Light Source, Paul Scherrer Institut, CH-5234 Villigen, Switzerland*

(Received 5 November 2004; published 8 August 2005)

The high-T_c superconductor $Tl_2Ba_2CuO_{6+\delta}$ is studied by angle-resolved photoemission spectroscopy. For a very overdoped $T_c = 30$ K sample, the Fermi surface consists of a single large hole pocket centered at (π, π) and is approaching a topological transition. Although a superconducting gap with $d_{x^2-y^2}$ symmetry is tentatively identified, the quasiparticle evolution with momentum and binding energy exhibits a marked departure from the behavior observed in under and optimally doped cuprates. The relevance of these findings to scattering, many-body, and quantum-critical phenomena is discussed.

DOI: 10.1103/PhysRevLett.95.077001 PACS numbers: 74.25.Jb, 74.72.Jt, 79.60.−i

Angle-resolved photoemission spectroscopy (ARPES) has provided crucial insights into the complex electronic structure of the high-T_c superconductors (HTSCs). However, unresolved issues remain partly because most of the ARPES data on cuprates have been obtained on a limited set of materials, such as $La_{2-x}Sr_xCuO_4$ (LSCO) and the single and double CuO_2 layer Bi cuprates (Bi2201 and Bi2212), whose electronic structure is complicated by several materials issues. These include chemical and particularly cation disorder, as well as family-specific problems: lattice distortions and spin/charge instabilities in LSCO; superstructure modulations and CuO_2 multilayer band splitting in the Bi cuprates [1].

Important breakthroughs may come from the study by ARPES of the Tl cuprates and, in particular, single layer $Tl_2Ba_2CuO_{6+\delta}$ (Tl2201). Owing to a well-ordered crystal structure with very flat CuO_2 planes far apart from each other, its electronic structure should be free of many complications found in other cuprates. Its $T_c^{\max} \simeq 93$ K is one of the highest among single layer materials: $T_c^{\max} < 40$ K for Bi2201 and LSCO, possibly due to structural effects or to larger and/or more harmful cation disorder [2]. Most importantly, Tl2201 can be synthesized over a wide doping range, from the optimal to the very overdoped regime. Although the latter is accessible in LSCO and Pb-doped Bi cuprates, these systems are affected by the cation disorder associated with Sr and Pb doping. Thus Tl2201 offers a unique opportunity to reach the heavily overdoped side of the cuprate phase diagram, where important hints of Fermi liquid behavior were obtained [3]. As most of the research effort has focused on the optimal and overdoped regime, in an attempt to understand the connection between Mott-Hubbard insulating behavior and superconductivity, the study of heavily overdoped Tl2201 represents an important alternative approach. At this stage, it has already been established that near optimal doping Tl2201 exhibits a few key features common to most cuprates, such as a $d_{x^2-y^2}$ superconducting (SC) gap [4] and the (π, π) magnetic resonant mode [5]. Additionally, in the very overdoped regime a coherent three-dimensional Fermi surface (FS) was recently observed in angular magnetoresistance oscillations measurements (AMRO) [6].

Unfortunately, ARPES experiments on Tl2201 have been severely hampered by the low-quality and/or short lifetime of the cleaved surfaces, which resulted in poorly resolved spectroscopic features. In this Letter, we present the first extensive ARPES study of high-quality single crystals of overdoped Tl2201 [7]. These results provide us with detailed information on FS and quasiparticle (QP) dispersion. While a SC gap consistent with $d_{x^2-y^2}$ symmetry is observed, the ARPES line shapes exhibit an unexpected momentum dependence: contrary to the case of under and optimally doped cuprates [1,8,9], QPs are sharp near $(\pi, 0)$, i.e., the *antinodal* region where the gap is maximum, and broad at $(\pi/2, \pi/2)$, i.e., the *nodal* region where the gap vanishes. In addition, while the QP linewidth at $(\pi/2, \pi/2)$ increases as a function of binding energy (E_B), in the $(\pi, 0)$ region it is sharper at the bottom of the band than closer to the Fermi energy (E_F).

ARPES experiments were carried out at the Swiss Light Source on the SIS beam line with a Scienta 2002 analyzer, circularly polarized 59 eV photons, and energy/angular resolutions of $\sim$24 meV/0.2°. Tl2201 single crystals were grown by a copper-rich self-flux method [7], with stoichiometry $Tl_{1.88(1)}Ba_2Cu_{1.11(2)}O_{6+\delta}$ corresponding to Cu substitution on the Tl site, thus away from the CuO_2 planes [10]. After careful annealing in controlled oxygen partial pressure, overdoped samples with T_c from 5 to 90 K were obtained; their high quality is evidenced by the narrow SC transitions, e.g., $\Delta T_c \simeq 0.7$ K for $T_c = 67$ K. The ARPES data were acquired in first and second Brillouin zones (BZs), returning analogous features, on two overdoped samples with $T_c = 63$ and 30 K (Tl2201-OD63; Tl2201-OD30). The samples, cleaved at 10 K and 6×10^{-11} torr, were kept at 10 K at all times.

Typical ARPES data from Tl2201-OD30 are presented in Fig. 1 together with the FS obtained from our band structure calculations within the local density approxima-

 © 2005 The American Physical Society

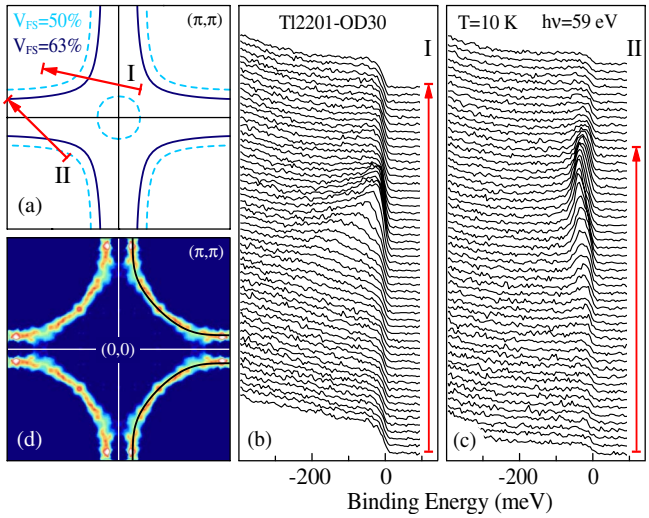

FIG. 1 (color online). (a) LDA FS for two different doping levels corresponding to a volume, counting holes, of 50% (cyan, dashed line) and 63% (blue, solid line) of the BZ. (b),(c) ARPES spectra taken at $T = 10$ K on Tl2201-OD30 along the directions marked by arrows in (a). (d) ARPES FS of Tl2201-OD30 along with a tight-binding fit of the data (black lines).

tion (LDA), which are in good agreement with previous calculations [11,12], and a tight-binding fit of the experimentally determined FS. The spectra in Figs. 1(b) and 1(c) were measured along momentum space directions near the nodal and antinodal regions of the BZ, as indicated by the arrows in Fig. 1(a). Dispersive features are clearly observable, with a behavior which is ubiquitous among the cuprates [1]. Close to the nodal direction the QP peak exhibits a pronounced dispersion that can be followed over ~250 meV below E_F; near $(\pi, 0)$, on the other hand, the band is much shallower with a van Hove singularity ~39 meV below E_F. By integrating over a ±5 meV window about E_F the ARPES spectra normalized at high binding energies, one obtains an estimate for the normal-state FS [Fig. 1(d); the E_F-intensity map across two BZs was downfolded to the reduced zone scheme and symmetrized with respect to the BZ diagonal, taking an average for equivalent k points, and then fourfolded]. As discussed later, at $T = 10$ K a d-wave SC gap is open along the FS; thus this procedure returns the loci of minimum excitation energy across the gap, which, however, still correspond to the underlying normal-state FS crossings [1].

The FS of Tl2201-OD30 [Fig. 1(d)] consists of a large hole-pocket centered at (π, π), which, as suggested by the low binding energy of the van Hove singularity [Fig. 1(c)], appears to be approaching a topological transition from hole to electronlike. The FS volume, counting holes, is $63 \pm 2\%$ of the BZ corresponding to a carrier concentration of 1.26 ± 0.04 hole/Cu atom, in very good agreement with Hall-coefficient [13] and AMRO [6] experiments, which found 1.30 and 1.24 itinerant holes, respectively, in slightly more overdoped samples. These measurements all indicate that the low-energy electronic structure of very overdoped Tl2201 is dominated by a single CuO band. In both ARPES and AMRO data there is no evidence for the TlO band that in LDA calculations crosses E_F and gives rise to a small electron pocket centered at $k = (0, 0)$ for nonoxygenated (i.e., $\delta = 0$) Tl2201 [Fig. 1(a), dashed FS]. This, however, is no surprise even within the independent particle picture. In fact, adjusting the chemical potential in the calculations in a rigid-band-like fashion to match the doping level of our Tl2201-OD30 sample (as determined by the total FS volume), the TlO band is emptied of its electrons and the LDA FS reduces to the single CuO pocket [Fig. 1(a), solid FS]. Since full depletion of the TlO band takes place for $\Delta E_F \simeq -0.159$ eV, corresponding to the removal of 0.024 electrons from the TlO band (as well as 0.109 from the CuO band), already the deviation of the Tl^{3+} and Cu^{2+} content of our samples from the stoichiometric ratio 2:1, which contributes ~0.14 hole/formula unit, would be sufficient to empty the TlO band even in the nonoxygenated $\delta = 0$ case. In this sense, the Tl-Cu nonstoichiometry and the presence of the TlO band cooperate in pushing the $\delta = 0$ system away from half filling, which may help explain why nonoxygenated Tl2201 is not a charge transfer insulator like undoped (i.e., $x = 0$) LSCO [12]. As for the detailed shape of the FS, which in LDA calculations is more square than in ARPES and AMRO results, better agreement would require the inclusion in the calculations of correlation effects and/or O-doping beyond a rigid-band picture. Alternatively, the ARPES data can be modeled by the tight-binding dispersion $\epsilon_{\mathbf{k}} = \mu + \frac{t_1}{2}(\cos k_x + \cos k_y) + t_2 \cos k_x \times \cos k_y + \frac{t_3}{2}(\cos 2k_x + \cos 2k_y) + \frac{t_4}{2}(\cos 2k_x \cos k_y + \cos k_x \times \cos 2k_y) + t_5 \cos 2k_x \cos 2k_y$, as in Ref. [14] (setting $a = 1$ for the lattice constant). With parameters $\mu = 0.2438$, $t_1 = -0.725$, $t_2 = 0.302$, $t_3 = 0.0159$, $t_4 = -0.0805$, and $t_5 = 0.0034$, all expressed in eV, this dispersion reproduces both the FS shape [Fig. 1(d)] and the QP energy at $(0, 0)$ and especially near $(\pi, 0)$ [Figs. 2(f) and 2(g)].

The analysis of the ARPES spectra in Fig. 2 indicates a SC gap consistent with a $d_{x^2-y^2}$ form. Because of the lack of normal-state data, the opening of the gap for this Tl2201-OD30 sample could not be followed via the shift of the leading edge midpoint (LEM) across T_c, as is commonly done (this was, however, possible in subsequent temperature dependent experiments on a less overdoped $T_c = 74$ K sample). In the present case, the existence of a gap can be most easily visualized by the comparison of nodal and antinodal symmetrized spectra [15], in particular, by the presence of a peak at E_F along the nodal direction [signature of a FS crossing; bold line in Fig. 2(a)] and by the lack thereof along the antinodal [Fig. 2(b)]. For a more quantitative analysis, we performed a fit of the spectra along different k-space cuts intersecting the underlying normal-state FS [Fig. 2(d); as line shape we used a Lorentzian QP peak plus a steplike background identified by the ARPES intensity at $k \gg k_F$, all multiplied by a Fermi function and convoluted with the instrumental en-

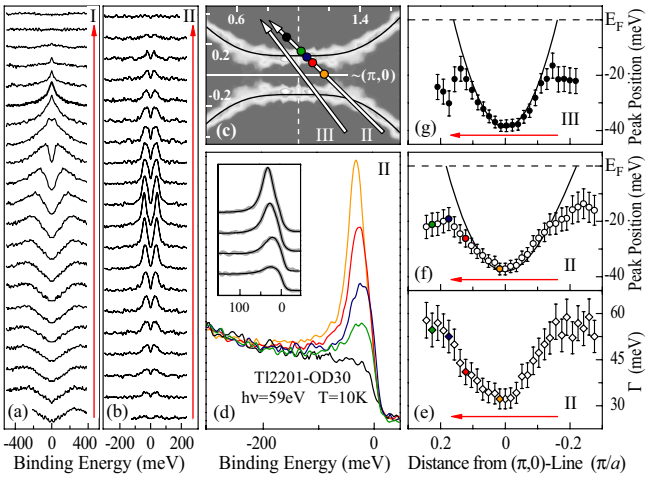

FIG. 2 (color online). (a),(b) Symmetrization of the ARPES spectra from along cuts I and II in Fig. 1. (c) Enlarged view of the FS of Tl2201-OD30 near $(\pi, 0)$. (d) Selected spectra from along cut II in (c); their k-space positions are indicated by circles of corresponding color. (e),(f) QP linewidth Γ and peak position from a Lorentzian fit of the energy distribution curves along cut II in (c). (g) Similarly, QP peak position along cut III in (c). Black lines in (c),(f),(g) are the tight-binding fit results.

ergy resolution function [1]]. As shown in Figs. 2(f) and 2(g), where the fit results are compared to our tight-binding dispersion for antinodal cuts II and III, the QP peak does not reach E_F when approaching k_F; instead it disperses back to higher binding energies losing intensity after having reached a minimum value $\simeq 17$ meV. This behavior is a hallmark of Bogoliubov QPs, and reveals the opening of a SC gap near $(\pi, 0)$. Because of the finite temperature and limited resolution of the experiment, the LEM of the k_F antinodal spectra is located at $\simeq 2$ meV above E_F. Our fitting procedure and detailed simulations by Kordyuk *et al.* [16], for comparable experimental parameters, suggest that the observed location of the LEM is consistent with the presence of a SC gap $\Delta \simeq 8$ meV; this gap value is a factor ~ 2 smaller than the QP peak position, as empirically noted for most HTSCs [1]. Along cuts intersecting the FS at the nodes (not shown), the fitting procedure indicates that the QP peak does cross E_F, while at intermediate momenta it returns a gap smaller than at the antinodes [Fig. 2(f), right-hand side of cut II].

Let us now consider the momentum evolution of the QP line shapes. A superficial inspection of the data in Figs. 1(b) and 1(c) shows that QPs are much broader in the nodal than in the antinodal region. Furthermore, while in the nodal region the width of the QP peak increases as a function of binding energy [Fig. 1(b)], as expected from phase space arguments, in the antinodal region the sharpest peak is found at the bottom of the band [Fig. 2(e)]. In Fig. 3(a) we present a compilation of spectra taken along the FS contour but at k slightly smaller than k_F and corresponding to a QP with $E_B \sim 35$ meV [this choice being dictated by the need to compare QP line shapes not affected by the presence of a d-wave gap and/or the anomalous low-energy broadening shown in Fig. 2(e)]. One can observe a sharp QP peak near $(\pi, 0)$, which becomes progressively broader upon going towards $(\pi/2, \pi/2)$. To qualitatively characterize the evolution of the QP component of the spectral weight, we subtract from the spectra the background taken at $k \gg k_F$ as in Fig. 3(b) [1,17]. Then we plot, as a function of the FS angle, the integrated spectral weight normalized to the near-$(\pi, 0)$ value [Fig. 3(c)] and the QP linewidth Γ estimated from the FWHM of the remaining QP component [Fig. 3(d)]. The low-energy spectral weight decreases monotonically along the FS in going from the antinodal to the nodal region and, correspondingly, the linewidth increases from ~ 50 to 180 meV. However, the spectral weight integrated over an energy window of ~ 550 meV is independent of the FS angle, so this seeming k-dependent loss of QP coherence is intrinsic and is not simply a decrease of intensity due to, e.g., matrix element effects.

In order to put these observations into a broader context, we should recall that in underdoped cuprates QPs are sharp near $(\pi/2, \pi/2)$ and ill defined around $(\pi, 0)$, in the normal state. Upon increasing doping, the antinodal QPs sharpen up, although they remain broader than the nodal QPs all the way to optimal doping. Even in the SC state, in which case the QPs gain considerable coherence at all momenta and especially in the antinodal region, the scattering rates determined by ARPES are still highly anisotropic with a minimum at $(\pi/2, \pi/2)$ [1]. At variance with this well established picture and the expectation that the elementary excitations should become simply more isotropic upon overdoping, the SC state results from Tl2201-OD30 show a reverse nodal/antinodal QP anisotropy [Figs. 3 and 4(b)]. A smaller anisotropy of this sort is also observed on less overdoped Tl2201-OD63 [Fig. 4(a)], indicating a trend

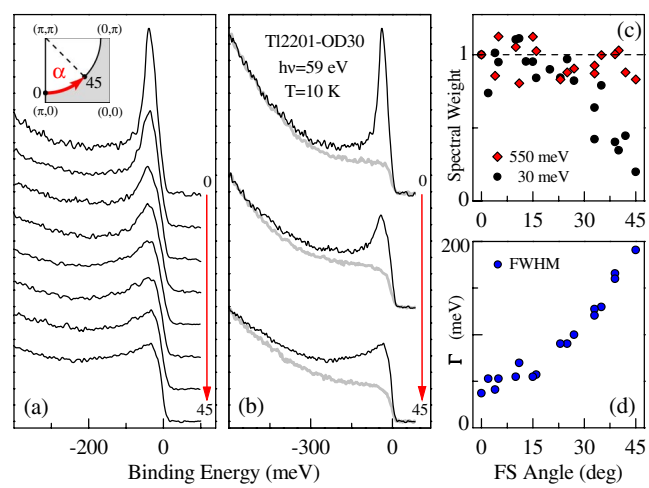

FIG. 3 (color online). (a) Tl2201-OD30 ARPES spectra at k slightly smaller than k_F (QPs with $E_B \sim 35$ meV) at various FS angles α. (b) Selected spectra from (a) along with corresponding $k \gg k_F$ background. (c),(d) Spectral weight integrated over different energy ranges and QP linewidth Γ, plotted vs α.

with overdoping. As a matter of fact, recent ARPES data from overdoped $x = 0.22$ LSCO [8,9] are qualitatively comparable to those from Tl2201-OD63 (for both systems $T_c \simeq \frac{2}{3} T_c^{\max}$), suggesting that this behavior might be generic to the overdoped cuprates.

Is this *QP anisotropy reversal* observed across optimal doping a signature of a quantum-critical point within the SC dome [18]? Interestingly, it was proposed that the proximity to a quantum phase transition from a $d_{x^2-y^2}$ to a $d_{x^2-y^2} + id_{xy}$ superconductor as a function of some parameter, possibly but not necessarily doping, may give rise to enhanced scattering of the gapless nodal QPs due to their coupling to a low-energy bosonic mode condensing at the phase transition [19]. However, while an id_{xy} pairing component leads to a state with no gapless fermionic excitations, the results from Tl2201-OD30 do not show a gap in the nodal region. This, together with thermal conductivity experiments [3], seems to indicate that the quantum criticality, if any, is not associated with the development of an id_{xy} pairing component or, perhaps, that doping is not the actual tuning parameter.

Alternatively, since a strongly k-dependent scattering rate is not supported by magnetotransport results (as suggested by the small low-T magnetoresistance, and by the comparison of low-T resistivity and cotangent of the Hall angle [13]), one may have to consider ARPES-specific QP broadening mechanisms, such as elastic forward scattering or residual k_z electronic dispersion. The latter may give rise to $k_{\|}$-dependent broadening of the ARPES features [20], especially in overdoped Tl2201 for which a 0.4% c-axis reduction with respect to optimal doping was reported [10] and a three-dimensional coherent electronic behavior was observed [6]. However, the c-axis dispersion vanishes at both nodal and antinodal points [6,20], which makes a connection between observed QP anisotropy and finite k_z dispersion not straightforward. Elastic small-angle (forward) scattering, due to n_i out-of-plane extended impurities such as cation substitution or interstitial oxygen, contributes a term $\Gamma_{\mathbf{k}_F} \propto (n_i V_0^2)/(v_{\mathbf{k}_F} \kappa^3)$ to the total normal-state electronic scattering (in the limit of large κ^{-1}, with V_0 and κ^{-1} being strength and range of the impurity potential [21]). Above T_c, $\Gamma_{\mathbf{k}_F}$ is larger at the antinodes due to the smaller Fermi velocity $v_{\mathbf{k}_F}$. Below T_c, however, due to energy conservation and the opening of the gap, $\Gamma_{\mathbf{k}_F}$ is strongly suppressed in the antinodal but not in the nodal region, where small-angle scattering is still pair-breaking [21]. This might provide an explanation for the anomalous k dependence of the QP scattering seen below T_c on overdoped Tl2201. As for the doping dependence in Fig. 4, one might speculate that while the broadening of the nodal QPs with doping is due to the increase of n_i (i.e., oxygen content) and in turn of $\Gamma_{\mathbf{k}_F}$, the sharpening of the antinodal QPs reflects a decrease of electronic correlations. On the other hand, the anomalous energy dependence of the $(\pi, 0)$ scattering rate in Fig. 2(e) does not seem to be accounted for and might actually be indicative of a distribution in gap magnitude due to electronic inhomogeneity, similar to what was previously reported for Bi2212 [22].

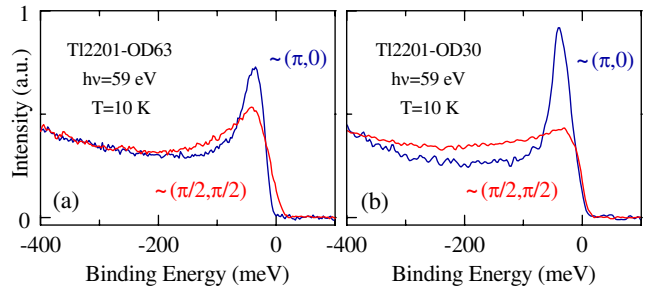

FIG. 4 (color online). (a) Tl2201-OD63 and (b) Tl2201-OD30 spectra at $k \lesssim k_F$ in the nodal and antinodal regions.

In conclusion, overdoped Tl2201 is the first HTSC for which a surface-sensitive single-particle spectroscopy and comparable bulk transport measurements have arrived at a quantitative agreement on a major feature such as the normal-state FS. As for the observed QP anisotropy reversal and its connection to various QP broadening scenarios, including the recent proposal for an increase of antinodal lifetime through multiple scattering off a single impurity [23], a more systematic study is required.

We thank K. M. Shen, D. G. Hawthorn, N. J. C. Ingle, N. E. Hussey, A. P. Mackenzie, M. Franz, D. J. Scalapino, and G. A. Sawatzky for discussions. This work was supported by the CRC Program, NSERC, CIAR, and BCSI.

[1] A. Damascelli *et al.*, Rev. Mod. Phys. **75**, 473 (2003).
[2] H. Eisaki *et al.*, Phys. Rev. B **69**, 064512 (2004).
[3] C. Proust *et al.*, Phys. Rev. Lett. **89**, 147003 (2002).
[4] C. C. Tsuei *et al.*, Nature (London) **387**, 481 (1997).
[5] H. He *et al.*, Science **295**, 1045 (2002).
[6] N. E. Hussey *et al.*, Nature (London) **425**, 814 (2003).
[7] D. C. Peets *et al.*, cond-mat/0211028.
[8] T. Yoshida *et al.*, Phys. Rev. Lett. **91**, 027001 (2003).
[9] X. J. Zhou *et al.*, Phys. Rev. Lett. **92**, 187001 (2004).
[10] Y. Shimakawa *et al.*, Phys. Rev. B **42**, 10 165 (1990).
[11] D. R. Hamann and L. F. Mattheiss, Phys. Rev. B **38**, R5138 (1988).
[12] D. J. Singh and W. E. Pickett, Physica (Amsterdam) **203C**, 193 (1992).
[13] A. P. Mackenzie *et al.*, Phys. Rev. B **53**, 5848 (1996).
[14] M. R. Norman, Phys. Rev. B **63**, 092509 (2001).
[15] M. R. Norman *et al.*, Nature (London) **392**, 157 (1998).
[16] A. A. Kordyuk *et al.*, Phys. Rev. B **67**, 064504 (2003).
[17] A. Kaminski *et al.*, Phys. Rev. B **69**, 212509 (2004).
[18] J. L. Tallon and J. W. Loram, Physica (Amsterdam) **349C**, 53 (2001).
[19] M. Vojta, Y. Zhang, and S. Sachdev, Phys. Rev. Lett. **85**, 4940 (2000).
[20] S. Sahrakorpi *et al.*, cond-mat/0501500.
[21] L. Zhu, P. J. Hirschfeld, and D. J. Scalapino, Phys. Rev. B **70**, 214503 (2004).
[22] S. H. Pan *et al.*, Nature (London) **413**, 282 (2001).
[23] K. Wakabayashi *et al.*, cond-mat/0504240.